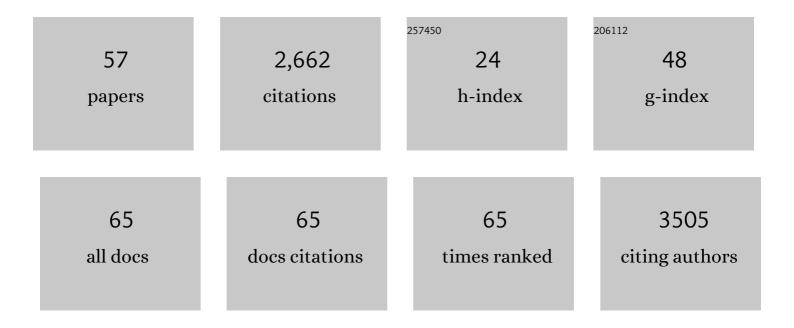
## Timothy A Whitehead

List of Publications by Year in descending order

Source: https://exaly.com/author-pdf/8701883/publications.pdf Version: 2024-02-01



| #  | Article   | IF   | CITATIONS |
|----|---|------|-----------|
| 1  | Computational Design of Proteins Targeting the Conserved Stem Region of Influenza Hemagglutinin.<br>Science, 2011, 332, 816-821.  | 12.6 | 527       |
| 2  | Optimization of affinity, specificity and function of designed influenza inhibitors using deep sequencing. Nature Biotechnology, 2012, 30, 543-548.   | 17.5 | 342       |
| 3  | Community-Wide Assessment of Protein-Interface Modeling Suggests Improvements to Design<br>Methodology. Journal of Molecular Biology, 2011, 414, 289-302.   | 4.2  | 131       |
| 4  | Plasmid-based one-pot saturation mutagenesis. Nature Methods, 2016, 13, 928-930.  | 19.0 | 130       |
| 5  | Trade-offs between enzyme fitness and solubility illuminated by deep mutational scanning.<br>Proceedings of the National Academy of Sciences of the United States of America, 2017, 114, 2265-2270. | 7.1  | 114       |
| 6  | Single-mutation fitness landscapes for an enzyme on multiple substrates reveal specificity is globally encoded. Nature Communications, 2017, 8, 15695.  | 12.8 | 102       |
| 7  | Lignin triggers irreversible cellulase loss during pretreated lignocellulosic biomass saccharification. Biotechnology for Biofuels, 2014, 7, 175.   | 6.2  | 90        |
| 8  | Deep sequencing methods for protein engineering and design. Current Opinion in Structural Biology,<br>2017, 45, 36-44.  | 5.7  | 88        |
| 9  | Minimal protein-folding systems in hyperthermophilic archaea. Nature Reviews Microbiology, 2004, 2, 315-324.  | 28.6 | 68        |
| 10 | The Interrelationship between Promoter Strength, Gene Expression, and Growth Rate. PLoS ONE, 2014,<br>9, e109105.   | 2.5  | 67        |
| 11 | Rapid Fine Conformational Epitope Mapping Using Comprehensive Mutagenesis and Deep Sequencing.<br>Journal of Biological Chemistry, 2015, 290, 26457-26470.  | 3.4  | 67        |
| 12 | High-Resolution Sequence-Function Mapping of Full-Length Proteins. PLoS ONE, 2015, 10, e0118193.  | 2.5  | 57        |
| 13 | Transcriptional profiling of the hyperthermophilic methanarchaeon Methanococcus jannaschii in response to lethal heat and non-lethal cold shock. Environmental Microbiology, 2005, 7, 789-797.      | 3.8  | 56        |
| 14 | Comprehensive Sequence-Flux Mapping of a Levoglucosan Utilization Pathway in <i>E. coli</i> . ACS<br>Synthetic Biology, 2015, 4, 1235-1243.   | 3.8  | 51        |
| 15 | Hotspot-Centric De Novo Design of Protein Binders. Journal of Molecular Biology, 2011, 413, 1047-1062.  | 4.2  | 41        |
| 16 | Computational Design of Novel Protein Binders and Experimental Affinity Maturation. Methods in Enzymology, 2013, 523, 1-19.   | 1.0  | 38        |
| 17 | Paired heavy- and light-chain signatures contribute to potent SARS-CoV-2 neutralization in public antibody responses. Cell Reports, 2021, 37, 109771.   | 6.4  | 38        |
| 18 | Selfâ€renaturing enzymes: Design of an enzymeâ€chaperone chimera as a new approach to enzyme<br>stabilization. Biotechnology and Bioengineering, 2009, 102, 1316-1322.                              | 3.3  | 37        |

ΤΙΜΟΤΗΥ Α WHITEHEAD

| #  | Article   | IF   | CITATIONS |
|----|---|------|-----------|
| 19 | A filamentous molecular chaperone of the prefoldin family from the deep-sea hyperthermophile<br>Methanocaldococcus jannaschii. Protein Science, 2007, 16, 626-634.  | 7.6  | 36        |
| 20 | One-shot identification of SARS-CoV-2ÂS RBD escape mutants using yeast screening. Cell Reports, 2021, 36, 109627.   | 6.4  | 35        |
| 21 | Rapid biosensor development using plant hormone receptors as reprogrammable scaffolds. Nature<br>Biotechnology, 2022, 40, 1855-1861.  | 17.5 | 34        |
| 22 | Biotemplated Metal Nanowires Using Hyperthermophilic Protein Filaments. Small, 2009, 5, 2038-2042.  | 10.0 | 32        |
| 23 | Negatively Supercharging Cellulases Render Them Lignin-Resistant. ACS Sustainable Chemistry and Engineering, 2017, 5, 6247-6252.  | 6.7  | 32        |
| 24 | Tying up the loose ends: circular permutation decreases the proteolytic susceptibility of recombinant proteins. Protein Engineering, Design and Selection, 2009, 22, 607-613.   | 2.1  | 31        |
| 25 | Computational redesign of the lipid-facing surface of the outer membrane protein OmpA. Proceedings of the National Academy of Sciences of the United States of America, 2015, 112, 9632-9637.   | 7.1  | 30        |
| 26 | Haplotype-Phased Synthetic Long Reads from Short-Read Sequencing. PLoS ONE, 2016, 11, e0147229.   | 2.5  | 29        |
| 27 | Insights into cellulaseâ€lignin nonâ€specific binding revealed by computational redesign of the surface of green fluorescent protein. Biotechnology and Bioengineering, 2017, 114, 740-750.   | 3.3  | 25        |
| 28 | An Automated Data-Driven Pipeline for Improving Heterologous Enzyme Expression. ACS Synthetic<br>Biology, 2019, 8, 474-481.   | 3.8  | 24        |
| 29 | Data-driven engineering of protein therapeutics. Current Opinion in Biotechnology, 2019, 60, 104-110.   | 6.6  | 22        |
| 30 | Characterizing Protein-Protein Interactions Using Deep Sequencing Coupled to Yeast Surface Display.<br>Methods in Molecular Biology, 2018, 1764, 101-121.   | 0.9  | 21        |
| 31 | Determination of binding affinity upon mutation for type I dockerin–cohesin complexes from <scp><br/><i>C</i> </scp> <i>lostridium thermocellum</i> and <scp> <i>C</i> </scp> <i>lostridium<br/>cellulolyticum</i> using deep sequencing. Proteins: Structure, Function and Bioinformatics, 2016, 84,<br>1914-1928. | 2.6  | 19        |
| 32 | User-defined single pot mutagenesis using unamplified oligo pools. Protein Engineering, Design and<br>Selection, 2019, 32, 41-45.   | 2.1  | 19        |
| 33 | Producing Glucose 6-Phosphate from Cellulosic Biomass. Journal of Biological Chemistry, 2015, 290, 26638-26648.   | 3.4  | 17        |
| 34 | Impact of In Vivo Protein Folding Probability on Local Fitness Landscapes. Molecular Biology and Evolution, 2019, 36, 2764-2777.  | 8.9  | 16        |
| 35 | Removal and upgrading of lignocellulosic fermentation inhibitors by in situ biocatalysis and<br>liquidâ€liquid extraction. Biotechnology and Bioengineering, 2015, 112, 627-632.  | 3.3  | 15        |
| 36 | Rational shape engineering of the filamentous protein Î <sup>3</sup> prefoldin through incremental gene<br>truncation. Biopolymers, 2009, 91, 496-503.  | 2.4  | 14        |

Τιμοτην Α Whitehead

| #  | Article   | IF   | CITATIONS |
|----|---|------|-----------|
| 37 | Fine Epitope Mapping of Two Antibodies Neutralizing the <i>Bordetella</i> Adenylate Cyclase Toxin.<br>Biochemistry, 2017, 56, 1324-1336.  | 2.5  | 14        |
| 38 | Characterization of Individual Human Antibodies That Bind Pertussis Toxin Stimulated by Acellular<br>Immunization. Infection and Immunity, 2018, 86, .  | 2.2  | 13        |
| 39 | The importance and future of biochemical engineering. Biotechnology and Bioengineering, 2020, 117, 2305-2318.   | 3.3  | 13        |
| 40 | Controlling the Selfâ€Assembly of a Filamentous Hyperthermophilic Chaperone by an Engineered Capping<br>Protein. Small, 2008, 4, 956-960.   | 10.0 | 12        |
| 41 | Pro region engineering of nerve growth factor by deep mutational scanning enables a yeast platform for conformational epitope mapping of antiâ€NGF monoclonal antibodies. Biotechnology and Bioengineering, 2018, 115, 1925-1937. | 3.3  | 12        |
| 42 | Optimization of multi-site nicking mutagenesis for generation of large, user-defined combinatorial<br>libraries. Protein Engineering, Design and Selection, 2021, 34, .   | 2.1  | 10        |
| 43 | Saturation Mutagenesis Genome Engineering of Infective ΦX174 Bacteriophage <i>via</i> Unamplified<br>Oligo Pools and Golden Gate Assembly. ACS Synthetic Biology, 2020, 9, 125-131.   | 3.8  | 8         |
| 44 | Stabilization of the SARS-CoV-2 receptor binding domain by protein core redesign and deep mutational scanning. Protein Engineering, Design and Selection, 2022, 35, .   | 2.1  | 8         |
| 45 | Regulatory Approved Monoclonal Antibodies Contain Framework Mutations Predicted From Human Antibody Repertoires. Frontiers in Immunology, 2021, 12, 728694.   | 4.8  | 7         |
| 46 | A peptide mimic of an antibody. Science, 2017, 358, 450-451.  | 12.6 | 6         |
| 47 | A yeast surface display platform for plant hormone receptors: Toward directed evolution of new biosensors. AICHE Journal, 2020, 66, e16767.   | 3.6  | 6         |
| 48 | A Method for User-defined Mutagenesis by Integrating Oligo Pool Synthesis Technology with Nicking<br>Mutagenesis. Bio-protocol, 2020, 10, e3697.  | 0.4  | 5         |
| 49 | Identification of SARS-CoV-2ÂS RBD escape mutants using yeast screening and deep mutational scanning.<br>STAR Protocols, 2021, 2, 100869.   | 1.2  | 4         |
| 50 | An overview of methods for the structural and functional mapping of epitopes recognized by anti-SARS-CoV-2 antibodies. RSC Chemical Biology, 2021, 2, 1580-1589.  | 4.1  | 4         |
| 51 | A Closed Form Model for Molecular Ratchet-Type Chemically Induced Dimerization Modules.<br>Biochemistry, 2023, 62, 281-291.   | 2.5  | 4         |
| 52 | Feline Interleukin-31 Shares Overlapping Epitopes with the Oncostatin M Receptor and IL-31RA.<br>Biochemistry, 2020, 59, 2171-2181.   | 2.5  | 3         |
| 53 | High-throughput evaluation of synthetic metabolic pathways. Technology, 2016, 04, 9-14.   | 1.4  | 2         |
| 54 | Introduction to the Rosetta Special Collection. PLoS ONE, 2015, 10, e0144326.   | 2.5  | 2         |

| #  | Article   | IF   | CITATIONS |
|----|---|------|-----------|
| 55 | The inner workings of an enzyme. Science, 2021, 373, 391-392.   | 12.6 | 1         |
| 56 | Facile Assembly of Combinatorial Mutagenesis Libraries Using Nicking Mutagenesis. Methods in<br>Molecular Biology, 2022, , 85-109.  | 0.9  | 1         |
| 57 | Pro region engineering of nerve growth factor by deep mutational scanning enables a yeast platform<br>for conformational epitope mapping of anti-NGF monoclonal antibodies. Biotechnology and<br>Bioengineering, 0, , . | 3.3  | 0         |